Title

Macular crystalline inclusions in Sjögren-Larsson syndrome are dynamic structures that undergo remodeling.

Journal

Ophthalmic Genetics, 41(4)

Authors

Al-Holou, Shaza
Siefker, Edward
Fouzdar-Jain, Samiksha
et al.

Publication Date

2020-08-01

DOI

10.1080/13816810.2020.1776340

Peer reviewed

HHS Public Access

Author manuscript

Ophthalmic Genet. Author manuscript; available in PMC 2021 August 01.

Published in final edited form as:

Ophthalmic Genet. 2020 August ; 41(4): 381–385. doi:10.1080/13816810.2020.1776340.

Macular Crystalline Inclusions in Sjögren-Larsson Syndrome are Dynamic Structures that Undergo Remodeling

Shaza N. Al-Holou[1], **Edward Siefker**[2], **Samiksha Fouzdar-Jain**[1,2,3], **Donny W. Suh**[1,2,3], **William B. Rizzo**[2,3]

[1]Stanley M. Truhlsen Eye Institute, University of Nebraska Medical Center, Omaha, Nebraska 68105, USA

[2]Department of Pediatrics and Child Health Research Institute, University of Nebraska Medical Center, Omaha, Nebraska 68198 USA

[3]Children's Hospital and Medical Center, Omaha, Nebraska 68114, USA

Abstract

Background—Sjögren-Larsson syndrome (SLS) is a rare genetic neurocutaneous disease caused by mutations in *ALDH3A2* that results in deficiency of fatty aldehyde dehydrogenase and accumulation of fatty aldehydes and alcohols. The disease is associated with ichthyosis, spasticity, and intellectual disability. Patients exhibit a characteristic retinopathy with macular crystalline inclusions that first appear in early childhood and increase with age. Once formed, the inclusions are thought to be inert and irreversible. We sought to document how the crystalline inclusions change over time.

Materials and Methods—Serial retinal photographs of 4 SLS subjects (9–23 years old) were taken over a period of 1–3 years. Images were compared by visual inspection and analyzed using ImageJ/Fiji software to observe changes.

Results—Visual inspection of retinal photographs of SLS subjects taken over time demonstrated distinctive changes in crystalline inclusions. New inclusions were formed and some established inclusions regressed. These changes were conveniently demonstrated with software-based photographic image analysis.

Conclusions—We conclude that macular inclusions in SLS are not simply inert deposits, but are dynamic structures that form over time and are subject to remodeling. This conclusion provides new insight into the interplay between the metabolic defect and retinal pathology in SLS, and raises the potential for new therapeutic approaches to reverse some aspects of the maculopathy.

Correspondence: William B. Rizzo, MD, Department of Pediatrics, 985940 Nebraska Medical Center, Omaha, NE 68198-5940, NE, USA, Tel : 1+ 402-559-2560, Fax: 402-559-2540, wrizzo@unmc.edu.

Contributions of Authors: Manuscript preparation (SNA. WBR); Data Acquisition and analysis (SNA, SFJ, ES, DWS); Manuscript review and approval (all authors).

Disclosure of interest:

The authors report no conflicts of interest in this work. No funding source influenced the study design, data interpretation, or writing of this manuscript.

Keywords

fatty alcohol; fatty aldehyde; image analysis; maculopathy; A*LDH3A2*

Introduction

Sjögren-Larsson syndrome (SLS; OMIM 270200) is an autosomal recessive neurocutaneous disease characterized by ichthyosis, spasticity, intellectual disability, and a distinctive maculopathy with crystalline inclusions. SLS is caused by mutations in *ALDH3A2* that result in deficient activity of fatty aldehyde dehydrogenase and impaired metabolism of fatty aldehydes and alcohols (1). These lipids, or their metabolic products, are thought to be responsible for the symptoms (2).

On fundus examination of SLS patients, the most notable feature is macular degeneration with characteristic perifoveal crystalline inclusions, originally described as glistening white dots (3–5). The crystalline inclusions first appear in early childhood and increase with age (4). Optical coherence tomography reveals that the inclusions are localized to the inner plexiform, inner nuclear, and outer plexiform layers, as well as the nerve fiber layer (5,6).

The biochemical composition of the macular inclusions in SLS is not known. Longitudinal ophthalmologic studies in this disease have rarely been reported and it is not known whether the macular inclusions, once formed, are static deposits. In this study, we prospectively used serial retinal photography and image analysis to demonstrate that the macular inclusions in SLS are dynamic structures that appear and can even regress over time.

Material and methods

Subjects

We enrolled 4 subjects with SLS in a longitudinal natural history study at the University of Nebraska Medical Center after providing informed consent. Only subjects with follow-up of one year or more were included in the study. All subjects showed the typical symptoms of ichthyosis, spastic diplegia, and intellectual disability, and carried pathogenic mutations in *ALDH3A2*. Our Institutional Review Board approved this research and the study adhered to the tenets of the Declaration of Helsinki.

Fundus photography

Ophthalmic examinations and color fundus photography were performed with the P-200Tx (Optos, Dunfermline, Scotland) or the Visucam (Zeiss, Jena, Germany) instruments.

Retinal Image Analysis

Retinal images were imported into ImageJ/Fiji software (7). All images were scaled to a uniform height of 584 pixels. Images were then registered in TrakEM2 (8), by manual selection of vessel junctions as landmarks and an affine transformation. Next, we used MorphoLibJ (9) to segment inclusions. Bright inclusions and dark vessels were removed by a morphological opening of radius 8, followed by a morphological closing of radius 22. The

resulting image was used to pseudo-flat field transform the original image by division. This image was then normalized and a morphological top hat of radius 2 was applied to enhance small, bright features. Shanbhag thresholding (10) yielded the final images. Crystalline inclusions were then colorized to red in baseline images or green in follow up images. Images were merged by aligning vessels to observe changes in the macular inclusions. All images were treated in the identical fashion.

Results

We studied 4 SLS subjects from three unrelated families over a period of 1–3 years. Pedigrees and clinical characteristics are summarized in Figure 1 and Table 1, respectively. Subjects 2 and 3 were identical twins. All subjects carried compound heterozygous mutations in *ALDH3A2*. One subject was an adult and the others were children between 9 and 16 years old when first studied. Visual acuity was minimal-moderately impaired and intraocular pressures were normal. All subjects had variable degrees of photophobia.

Color fundus photography revealed macular crystalline deposits in the perifoveal regions bilaterally in all subjects (Figure 2, Subjects 2 and 4). Dozens of inclusions of varying sizes were present. The inclusions were scattered in a macular area corresponding to approximately 1- to-1.5 optic disk diameter. For each SLS subject, the pattern of inclusions was different in each eye but the number of inclusions appeared to be comparable. This observation also applied to Subjects 2 and 3, who were identical twins.

Visual comparison of baseline and follow up photographs revealed striking differences in appearance of some inclusions in photos taken 1–3 years apart (Figure 2). Some smaller inclusions first appeared during this time and others disappeared. Certain larger inclusions seemed to grow or merge with neighboring ones and persisted throughout the time interval studied.

To better identify changes in the macular inclusions over time, we processed the retinal photographs using ImageJ/Fiji software (see METHODS; Figure 3). Macular inclusions taken at baseline were colorized to red and inclusions at follow up exam were assigned green. Figure 4 shows image analysis of Subject 2 taken over a 2-year interval. The inclusions in the baseline image have a red color (Figure 4A) and inclusions in the follow up image are green (Figure 4B). When these two images were merged, the majority of inclusions were unchanged and appear yellow (Figure 4C). However, some red inclusions had regressed or disappeared entirely, whereas others (green) subsequently arose during the time interval between photographs. The remaining 3 SLS subjects demonstrated similar changes (not shown).

Discussion

By combining visual inspection of serial retinal photographs and a novel image analysis process, we detected alterations in macular crystalline inclusions in SLS subjects over time. New inclusions developed, and others appeared to regress and disappear entirely. These findings suggest that the inclusions are not simply inert deposits, but are dynamic structures that are subject to remodeling, at least to some extent. The inclusions first appear in early

childhood and increase in number with age (4,6). Our results suggest that the number of inclusions represents a balance between formation of new ones and elimination of older ones, with formation exceeding regression in childhood. We observed similar inclusion dynamics in our older 23-year-old SLS patient (Subject 1), suggesting that this process is also ongoing in adults. Further, the pattern of inclusions is not strictly determined by genotype, as our identical twin subjects demonstrated a different and individually unique pattern.

How some inclusions in SLS can be eliminated in patients with a persistent metabolic defect is not known. Even the smallest ones are much too large to be phagocytized by individual macrophages. Furthermore, little is known about the histological appearance of the inclusions. A single pathology report of one SLS eye, obtained postmortem from a 54-year-old SLS patient, found increased lipofuscin granules and melanin in the macular region without specifically identifying crystalline inclusions (11).

The composition of the macular inclusions in SLS is also not known. The genetic defect in SLS results in impaired breakdown of fatty aldehydes and fatty alcohols (1,2). These lipids and/or their metabolic products accumulate in cultured SLS cells and plasma (2,12). In addition, reactive oxygen species generated by photo-oxidative stress can attack polyunsaturated fatty acids and macular pigments in the retina, thereby generating potentially toxic fatty aldehydes that are not properly metabolized in SLS patients (1). It is therefore possible that the inclusions are composed of these types of stored lipids and/or related aldehyde-modified proteins and lipofuscin. Using spectral analysis of the retina, SLS patients have been shown to have a profound reduction in the macular pigments: lutein and zeaxanthin (13). Although the basis for this depletion is not yet known, macular pigments have powerful anti-oxidative properties and their deficiency in SLS is likely to increase risk for retinal damage from photo-oxidative stress (1).

Image analysis of the macular inclusions in SLS proved to be a convenient method for detecting changes in this disease. The method that we developed uses routine fundus photography coupled with freely available ImageJ/Fiji software and plug-ins. No sophisticated instrumentation was required. By extracting fine details of the images, including vessels and macular inclusions, we were able to focus on the inclusions specifically. This approach may be applicable for other retinal diseases with characteristic macular inclusions, such as macular telangiectasia type-2 (14).

Finally, the dynamic property of macular inclusions in SLS, with spontaneous resolution of some inclusions, raises the possibility that therapeutic interventions may effectively prevent or even reverse some aspects of the retinal pathology. With the development of new therapeutic approaches for SLS that address the primary metabolic error (2), routine fundus photography and image analysis should be particularly useful as a tool for monitoring clinical response.

Conclusion

Macular inclusions in SLS are dynamic structures that appear in childhood, increase in number but can even regress over time. This dynamic characteristic provides new insight into the macular inclusions in SLS and the potentially reversible nature of the retinal pathology.

Acknowledgments

We thank Joel Rivas for expert technical assistance with image acquisition. We gratefully acknowledge funding (grant U54 HD061939) from the Sterol and Isoprenoid Research Consortium of the Rare Disease Clinical Research Network, and from the *Eunice Kennedy Shriver* National Institutes of Child Health & Human Development and National Center for Advancing Translational Sciences, NIH. Funding was also provided by the Child Health Research Institute of the University of Nebraska Medical Center and Children's Hospital & Medical Center.

References

1. Fouzdar-Jain S, Suh DW, Rizzo WB. Sjögren-Larsson syndrome: a complex metabolic disease with a distinctive ocular phenotype. Ophthalmic Genet. 2019;40:298–308. [PubMed: 31512987]
2. Rizzo WB. Genetics and prospective therapeutic targets for Sjögren-Larsson Syndrome. Expert Opin Orphan Drugs. 2016;4:395–406. [PubMed: 27547594]
3. Jagell S, Polland W, Sandgren O. Specific changes in the fundus typical for the Sjögren-Larsson syndrome. An ophthalmological study of 35 patients. Acta Ophthalmol. 1980;58:321–30. [PubMed: 7415820]
4. Willemsen MAA., Cruysberg JR, Rotteveel JJ, et al. Juvenile macular dystrophy associated with deficient activity of fatty aldehyde dehydrogenase in Sjögren-Larsson syndrome. Am J Ophthalmol. 2000;130:782–89. [PubMed: 11124298]
5. Jack LS, Benson C, Sadiq MA, et al. Segmentation of retinal layers in Sjögren–Larsson syndrome. Ophthalmology. 2015;122:1730–30. [PubMed: 25784589]
6. Fuijkschot J, Cruysberg JRM, Willemsen MAAP, et al. Subclinical changes in the juvenile crystalline macular dystrophy in Sjögren–Larsson syndrome detected by optical coherence tomography. Ophthalmology. 2008;115:870–75. [PubMed: 17826835]
7. Schindelin J, Arganda-Carreras I, Frise E, et al. Fiji: an open-source platform for biological-image analysis. Nature Methods. 2012;9:676–682. [PubMed: 22743772]
8. Cardona A, Saalfeld S, Schindelin J, et al. TrakEM2 software for neural circuit reconstruction. PLoS One. 2012;7(6):e38011. [PubMed: 22723842]
9. Legland D, Arganda-Carreras I, Andrey P. MorphoLibJ: integrated library and plugins for mathematical morphology with ImageJ. Bioinformatics. 2016;32:3532–3534. [PubMed: 27412086]
10. Shanbhag AG. Utilization of information measure as a means of image thresholding. CVGIP: Graphical Models and Image Processing. 1994;56:414–419.
11. Nilsson SE, Jagell S. Lipofuscin and melanin content of the retinal pigment epithelium in a case of Sjögren-Larsson syndrome. Br J Ophthalmol. 1987;71:224–26. [PubMed: 3828281]
12. Rizzo WB, Craft DA. Sjögren-Larsson syndrome: accumulation of free fatty alcohols in cultured fibroblastsa and plasma. J Lipid Res. 2000;41:1077–81. [PubMed: 10884288]
13. van der Veen RL, Fuijkschot J, Willemsen MA, et al. Patients with Sjögren-Larsson syndrome lack macular pigment. Ophthalmology. 2010;117:966–77. [PubMed: 20163870]
14. Kovach JL, Isildak H, Sarraf D. Crystalline retinopathy: Unifying pathogenic pathways of disease. Surv Ophthalmol. 2019;64:1–29. [PubMed: 30144456]

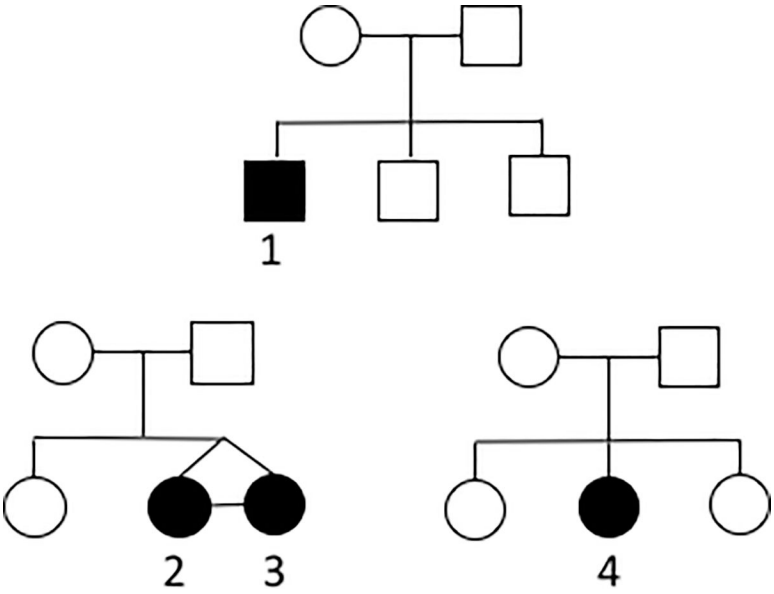

Figure 1.

Nuclear pedigrees of the SLS subjects studied. Numbers correspond to the subjects listed in Table 1. The ages at diagnosis of SLS were 8 months (Subject 1), 16 years (Subjects 2 and 3), and 19 months (Subject 4). Filled symbols correspond to affected SLS family members.

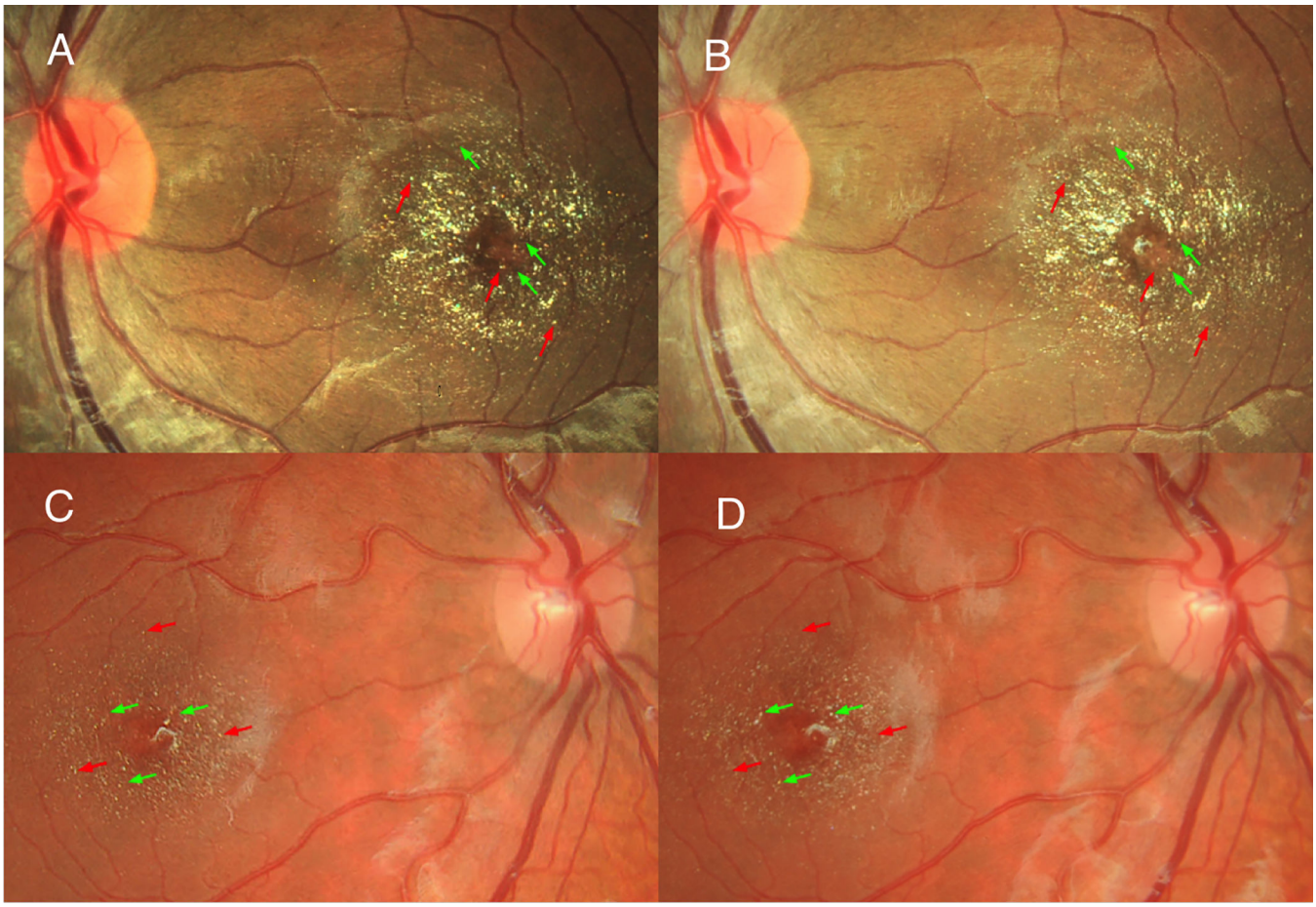

Figure 2.

Changes in retinal inclusions over time. Retinal photographs were taken from subject 2 (A, B) and Subject 4 (C, D). Subject 2 at baseline (A) and after 2-years (B), and Subject 4 at baseline (C) and after 1-year (D), demonstrate numerous changes. A, C: Red arrows point to examples of inclusions that have regressed over time in B and D, respectively; green arrows point to several inclusions that have newly appeared in B and D.

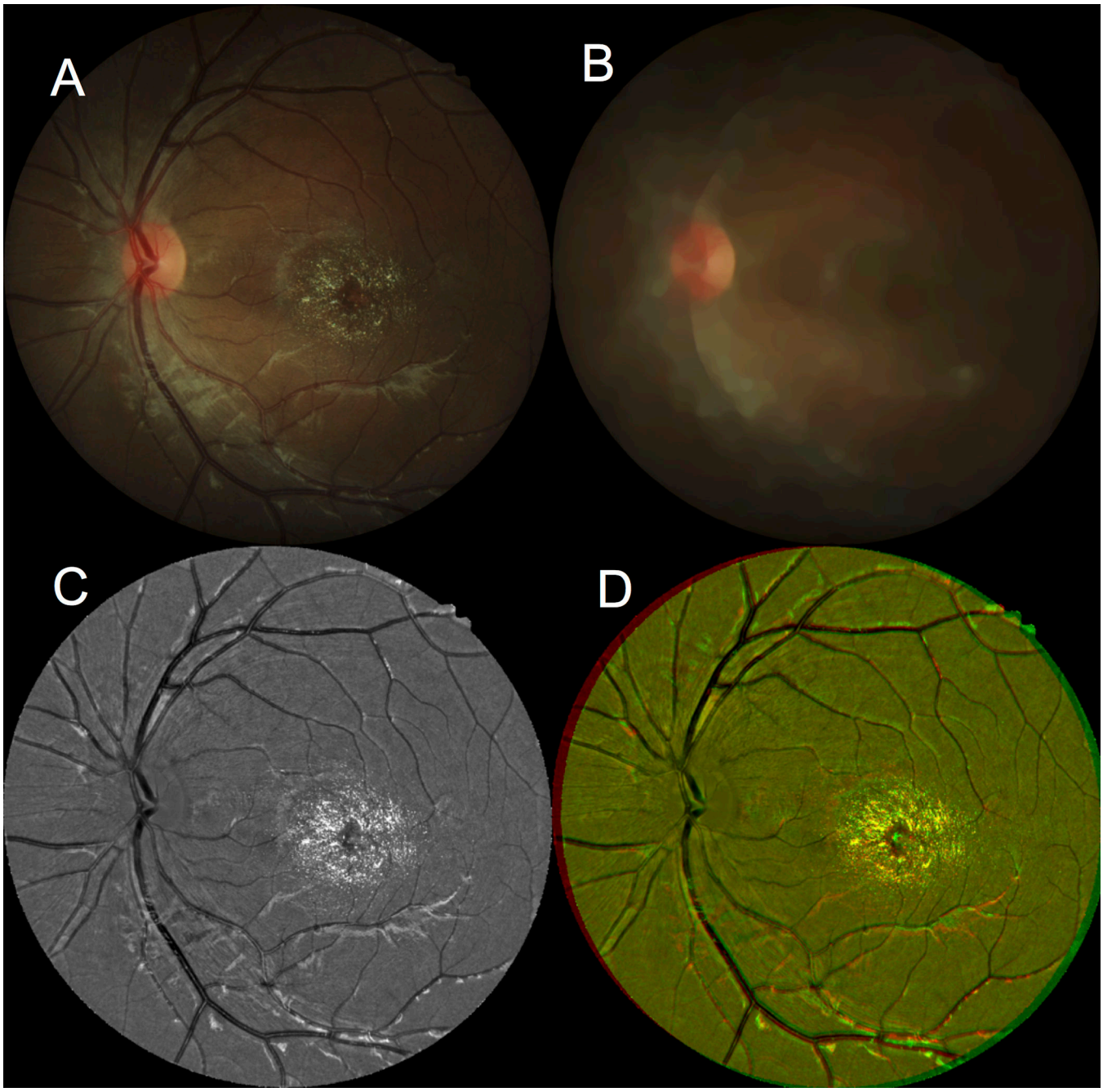

Figure 3.

Process used for image analysis of retinal inclusions. A: Original retinal image imported into ImageJ/Fiji software. B: Fine detail is extracted from the image, leaving behind depleted image. C: Fine detail including retinal inclusions is normalized for exposure and converted to black & white, which can be subsequently colorized. D: Baseline (red) and follow up (green) images are merged.

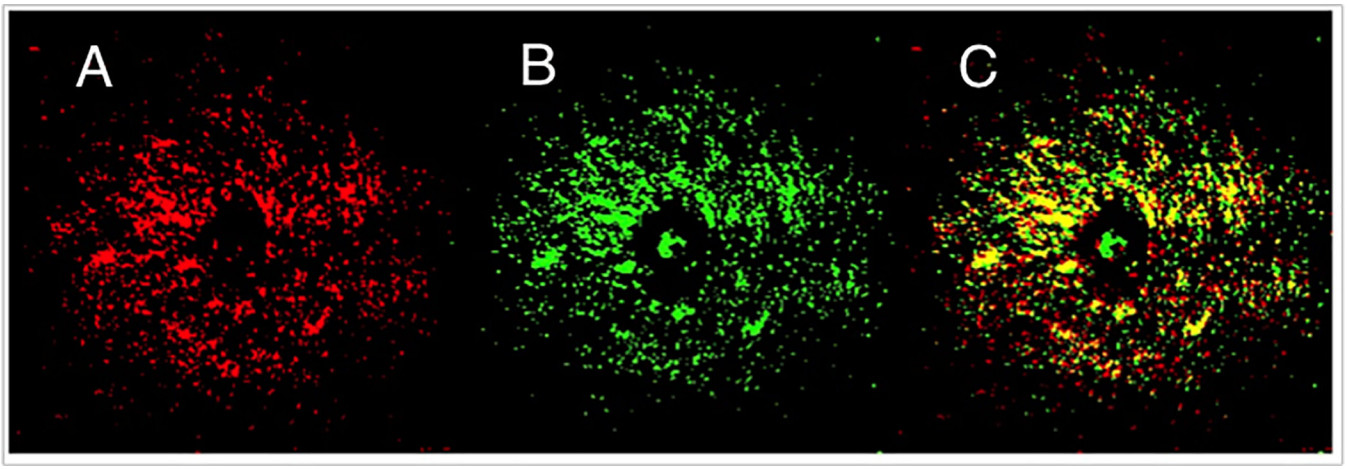

Figure 4.

Image analysis of macular inclusions. Subject 2 at baseline (A, red) and after 2 years (B, green). The merged image (C) reveals unchanged inclusions as yellow color; green inclusions are newly formed, and red inclusions have disappeared.

Table 1.

Characteristics of the SLS patients studied.

SLS Subject	Sex	*ALDH3A2* Genotype (Ethnicity)	Age at Baseline and Follow-up (yrs)	Visual Acuity	Intraocular Pressure (mm Hg)	Non-Ocular Features
1	Male	c.554G>C/ c.386–6A>G; c.1307_1311dupACAAA	23	20/60 OD, 20/60 OS	15 OD, 17 OS	Ichthyosis, spastic diplegia, intellectual disability, dysarthria, severe lower extremity contractures, non-ambulatory
		(Irish, French Canadian, American Indian)	26	20/40 OD, 20/70 OS	NR	
2	Female	c.191T>A/ c.374_378delCCATC (African American)	16	20/40 OD, 20/30 OS	19 OD, 19 OS	Ichthyosis, spastic diplegia, intellectual disability, dysarthria, ambulatory with braces
			18	NR	NR	
3	Female	c.191T>A/ c.374_378delCCATC (African American)	16	20/40 OD, 20/40 OS	15 OD, 19 OS	Ichthyosis, spastic diplegia, intellectual disability, dysarthria, ambulatory with braces
			18	NR	NR	
4	Female	c.407C>T/ 17p11.2 del [ch17:18,716,455_20,160,197] (Irish, English, American Indian)	9	20/100 OD, 20/100 OS	16 OD, 18 OS	Ichthyosis, spastic diplegia, intellectual disability, dysarthria, ambulatory with braces and crutches
			10	NR	NR	

Abbreviations: NR, not recorded.